1 Theory

1.1 Dislocation lines

Several investigations have documented that dislocations in silicon give rise to characteristic photoluminescence (PL) spectra below the band edge. First showed in [12] which labeled them D1 (0.812eV), D2 (0.875eV), D3 (0.934eV) and D4 (1.000eV). The samples where deformed at 850° C by bending, so that dislocation densities was inhomogeneous along the samples. [12] states that the intensity of theese lines increase when the dislocation-rich parts of the crystal is approached. At the same time the intensity of the intrinsic characteristics decrease. The distance between D1-D4 (62 ± 3 meV) corresponds to the energy of the optical phonons in silicon [12]. [12] reports D1 and D2 are dominant in heavily deformed Si crystals, while D3 and D4 predominate in weakly deformed Si. A similar result was also reported by recent study [20] for small angle grain boundaries using cathodoluminescence.

[26] suggest that D1-D4 are due to dislocations which have been frozen in under low-shear stress. Photoluminescence under uniaxial stress shows that D1/D2 originate in the tetragonal defect with random orientation relative to <100> directions. [26] conclude that D3 and D4 are closely related, whereas the independent D1/D2 centers might be deformation-produced point defects in the strain region of dislocations. New lines D5 and D6 emerge when high-temperature, low-stress deformation is followed by low-temperature, high-stress deformation. [26] propose that line D5 is due to straight dislocations and D6 is due to stacking faults. [26] also suggest that D3/D4 photoluminescence is much more characteristic of the dislocations themselves than the D1/D2 emission lines. [38] state that D5 is correlated with electron-hole recombination at localized centers on separate partial dislocations. After annealing at moderate temperatures (T > 360°C) the new lines merge into D4 [38].

The origin of D1 and D2 is not clear. It has been argued that they originate in electronic transition at the geometrical kinks on dislocations [29], point defects [26] and impurities [17] and/or from the reaction products of dislocations [27]. On the other hand, D3 and D4 lines is generally thought to be related to electronic transition within dislocation cores [19]. In addition, it has been suggested that the D3 line most likely is a phonon-assisted replica of D4 [19].

Both [12] and [26] studied plastically deformed silicon made by the Czochralski process (Cz-Si). [33] studied dislocations in multicrystalline silicon (mc-Si) and found similar lines with the entire set of D-lines shifted with around 10meV, presumably due to a strain field. Using a laser annealing technique,

[28], to introduce dislocations on a Cz-Si wafer, confirm the band location of D1-D4 from [26] in [33]. A principal difference between dislocation D'-lines in mc-Si versus D-lines in Cz-Si is a substantial broadening (60-70meV at 77K) of the D1'/D2' lines [33].

Cz-Si [12]	D1	D2	D3	D4
	0.812eV	0.875eV	0.934eV	1.000eV
mc-Si [33]	D1'	D2'	D3'	D4'
	0.80eV	0.89eV	0.95eV	1.00eV

Table 1: Energy positions of dislocation D-lines in Cz-Si and D' bands in mc-Si

[33] reveal a linear dependence of the band-to-band photoluminescence intensity and minority carrier lifetime across entire multicrystalline-Si wafers. Photoluminescence mapping in [33] of the 0.78eV (0.8eV) band intensity reveal a linkage to areas of a high dislocation density. This band should also be visible in room temperature [33].

[34] later found that if the contamination level is too low, or too high (dislocation decorated by metal silicate precipitates) the defect photoluminescence band vanished in room temperature. However, a relatively low contamination level of dislocations, in the order of 10 impurity atoms per micron of the dislocation length produces distinguishable defect band luminescence [34].

Dislocation related lines (D-lines) has been observed in low temperature photoluminiscence spectra from the regions which included the intragrain defects [31]. They also conclude that grain boundaries are not active recombination centers. [31] also show a TO-phonon replica of the boron bound exiton at 1.093eV. Intensity of boron bound exiton from the long lifetime regions was higher than that from the short lifetime regions. D-lines reported by [26] are in a short lifetime region. For a long lifetime region, [31] observe a peak at 1.00eV which is not the D4 line, but the zonecenter optical phonon sideband of the two-hole transition in the boron bound exiton [10]. There have been no reports on the D-line spectrum missing only the D1 line [31].

[2] demonstrate three areas of a sample with only D3 and D4 present. [2] conclude that this is due low concentration of metallic impurities.

[30] study origins of the defects by low temperature photoluminescence spectroscopy, electron backscatter diffraction pattern measurement and the etch-pit observation, and conclude that defects are metal contaminated dislocation clusters which originated from small angle grain boundaries.

1.2 Impurities

Diffusion of transition metals into silicon crystals result in a variety of different electrically active levels in the forbidden bandgap.

1.2.1 Atom impurities

Early work done by [10] compare intrinsic silicon from the Czochralski process with doped silicon. [10] do extensive photoluminescence study with doping atoms As, P, Sb, Bi, B, Ga, In and Al. The high intensity transverse optical lines occur at 1.0907eV, 1.0916eV, 1.0921eV, 1.0888eV, 1.0924eV, 1.0914eV, 1.0835eV and 1.092eV respectively with the different doping atoms present. Impurities like carbon complexes with many impurities in silicon, resulting in a large variety of photoluminescence centers. Detected complexes are another C atom, one oxygen atom, one N atom, one Ga atom, the four-lithium atom complex, beryllium and numerous radiation damage centres, especially involving oxygen [9]. See appendix 2 for energies.

Titanium photoluminescence has been observed around 2.85eV in 4H silicon carbide by [25], and in 6H by [35] at 2.79eV, 2.82eV and 2.86eV named ABC lines.

Interstitial chromium doesn't give any specific photoluminescence spectra for wavelengths up to 1800nm [7]. However, chromium bound with a boron atom can be identified as a peak around 0.85eV [7] [8].

Copper doping of silicon crystals results in an intense emission at 1.014eV [37]. [38] study Cu doped Si and observe a shoulder on the D1 line which presumably arises from Cu precipitates at the dislocation.

[6] introduce Fe atoms into a float-zone silicon crystal and observe a spectrum of 0.735eV which relate to a complex defect containing iron. Interstitial iron Fe, is about 10 times more effective as a recombination center than Fe-B pairs by low-level lifetime measurements and therefore reduces the minority carrier diffusion length more strongly [39].

Recent work in [13] show that micro-photoluminescence is an excellent tool for identifying metal precipitates in silicon. Iron images in [22] reveal internal gettering of iron to grain boundaries and dislocated regions during ingot growth. The minimum size for detection is 1μm, or even smaller, since the photoluminescence signal might be broadened. Precipitates from Fe and Cu are detected due to reduced band to band recombination intensity. Iron in silicon also affect the defect photoluminescence [13].

1.2.2 Impurities bound with doping atoms

Silicon samples containing chromium-boron pairs exhibit characteristic luminescence lines in the 0.84eV region where the intensity increased linearly with laser power [8].

[23] observe a luminescence spectra around 1.07eV in boron-doped, iron-diffused crystalline silicon and suggest the source is Fe-B pairs.

1.2.3 Interaction with dislocations

Investigation in [16] show that transition-metal contamination plays an important role in the production of D-band luminescence from silicon samples containing either epitaxial stacking faults or oxidation-induced stacking faults. [28] found that Cu doping resulted in reduced intensity of D1 and D2, and the intensity of D3 and D4 become very small. [38] demonstrate that a complete passivation of the D-band luminescence is achieved at higher Cu and Fe concentration when deliberately contaminating high purity silicon samples which contain dislocations. However impurities like Ni, lead to no detectable changes in the spectrum [38]. D-band recombination in Si is found to be independent of impurities trapped at dislocations [38], and [27] concluded that metallic impurities don't seem to be related to D1 and D2 luminescence. Even so, it is still generally accepted that metal impurity influence it. Metal precipitation at crystal defects during the crystal growth can clean grains from impurities, and thus improve the performance as suggested for iron in [4]. A recent example of interaction with defects is iron precipitates in [13], showing an enhanced defect photoluminescence at 1.3μm (0.95eV). The same study show that copper contamination almost completely suppress the defect photoluminescence. This is in agreement with [28]. Supression of defect photoluminescence by high copper concentrations was also reported in [21]. Cu precipitates can be located by reduced intensity of the band to band photoluminescence peak, both in areas with dislocations, and without [13].

Electron hole droplets (EHD), free excitons (FE) and bound excitons (BE) localized on phosphorus atoms has been steadily observed in [11] with photoluminescence on samples with low-dislocated regions. When increasing dislocation density the FE, BE and EHD bands decrease sharply. This may be due exciton capture by dislocation lines D1,D2 and non-radiative recombination [11]. EHD photoluminescence intensity is highly dependent on the pumping power [24]. There is a linear dependence, and pumping with 3mW or less makes it hardly visible in [24].

Room temperature mapping of the 0.77eV band is attributed to oxygen

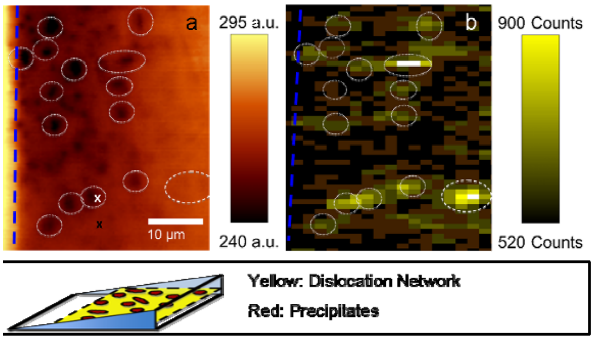

Figure 1: Bottom: Scheme of the sample preparation with the polished angle. Top: A Intensity of the BB PL peak at room temperature (a), and of the iron X-ray Kα fluorecence (b) from [13]. The dislocation network intersects the surface to the right of the dashed blue line. The white circles show recombination active precipitates.

precipitates in in thermally treated silicon made by the Czochralski process (Cz-Si) [32]. This band peak shifts parallel to the bandgap with temperature. The increase of this band on the dislocation lines is due to the preferential precipitation of oxygen [32].

[18] state that the deep-level emission from multicrystalline silicon with an intensity maximum at 0.78eV at room temperature is diffrent from that of the D1 line at low temperature. Furthermore, [18] suggest that the 0.78eV emission is associated with oxygen precipitation, and that the intra-grain defects are dislocation clusters decorated with oxygen impurities in addition to heavy-metal impurities. [14] state that the origin of trap densities in multicrystalline silicon could be structural crystal defects, which are highly decorated with oxygen precipitates.

References

[1] T. Arguirov, W.Seifer, G. Jia, and M. Kittler. Photoluminiscence study on defects multicrystalline silicon. *Semiconductors*, 2006.

[2] T. V. Arguirov. Electro-optical properties of dislocations in silicon and their possible application for light emmiters. ., 2007.

[3] Tz. Arguirov, W. Seifert, M. Kittler, and J. Reif. Temperature behaviour of extended defects in solar grade silicon investigated by photoluminescence and ebic. *Elsevier B.V.*, 2003.

[4] J. Bailey and E. R. Weber. Precipitation of iron in polycrystalline silicon. *Physica Status Solidi (a)*, 1993.

[5] S. Binetti, J Libal, M Acciarri, M. Di Sabatino, H. Nordmark, E.J. Øverlid, J.C. Walmsley, and R. Holmestad. Study of defects and impurities in multicrystalline silicon grown from metallurgical silicon feedstock. *Materials Science and Egnineering B*, 2008.

[6] M.I. Càlão and M.C. do Carmo. Luminescence from an iron related deep center in silicon. *Physica Scripta*, 1988.

[7] H. Conzelmann, K. Graff, and E.R. Weber. Chromium and chromium-boron pairs in silicon. *Appl. Phys. A*, 1982.

[8] H. Conzelmann and J. Weber. Photoluminescence from chromium-boron pairs in silicon. *Physica*, 1983.

[9] Gordon Davies. The optical properties of luminescence centres in silicon. *Physics Report*, 1988.

[10] P. J. Dean, J.R. Haynes, and W.F. Flood. New radiative recombination processes involving neutral donors and acceptors in silicon and germanium. *Physical Review Volume 161 Number 3*, 1967.

[11] N. Drozdov and A. Fedotov. Electron-hole drops in dislocational silicon. *Microelectronic Engineering 66*, 2002.

[12] N. A. Drozdov, A.A. Patrin, and V.D Tkachev. Recombination radiation on dislocations in silicon. *Pis'ma Xh. Eksp. Teor. Fiz.*, 1976.

[13] Paul Gundel, Martin C. Schubert, Wolfram Kwapil, Jonas Schön, Manfred Reiche, Hele Savin, Marko Yli-Koski, Juan Angel Sans ans Gema Martinez-Criado, Winfried Seifert, Wilhelm Warta, and Eicke R. Weber.

Micro-photoluminescence spectroscopy on metal precipitates in silicon. *Phys. Status Solidi RRL*, 2009.

[14] Paul Gundel, Martin C. Shubert, and Wilhelm Warta. Origin of trapping in multicrystalline silicon. *Journal of applied physics*, 2008.

[15] R.B. Hammond, TC. McGill, and J.W. Mayer. Temperature dependence of the electron-hole-liquid luminescence in si. *Physical Review B*, 1975.

[16] V. Higgs, M. Goulding, and P. Kightley. Characterization of epitaxial and oxidation-induced stacking faults in silicon: The influence of transition-metal contamination. *Appl. Phys. Lett.*, 1992.

[17] V. Higgs, P. Kightley, P.J. Goodhew, and P.D. Augustus. Metal-induced dislocation nucleation for metastable sige/si. *Appl. Phys. Lett.*, 1991.

[18] M. Inoue, H. Sugimoto, M. Tajima, Y. Ohshita, and A. Ogura. Microscopic and spectroscopic mapping of dislocation-related photoluminescence in multicrystalline silicon wafers. *J. Mater Sci*, 2007.

[19] V.V Kveder, E.A. Steinman, S.A. Shevchenko, and H.G. Grimmeiss. Dislocation-related electroluminescence at room temperature in plastically deformed silicon. *Phys. Rev. B*, 1995.

[20] Woong Lee, Jun Chen, Bin Chen, Jiho Chang, and Takashi Sekiguchi. Cathodoluminescence study of dislocation-related luminescence from small-angle grain boundaries in multicrystalline silicon. *Applied Physics Letters*, 2009.

[21] E. C. Lightowlers and V. Higgs. Luminescence associated with the presence of dislocations in silicon. *Physica Status Solidi (a)*, 1993.

[22] D. Macdonald, J. Tan, and T. Trupke. Imaging interstitial iron concentrations in boron-doped crystalline silicon. *Journal of applied physics*, 2008.

[23] H.D. Mohring, J. Weber, and R. Sauer. Photoluminescence of excitons bound to an isoelectronic trap in silicon associated with boron and iron. *Physical Review B*, 1983.

[24] Satoshi Nihonyanagi and Yoshihiko Kanemitsu. Enhanced luminescence from electron-hole droplets in silicon nanolayers. *Applied physics letters*, 2004.

[25] L. Patrick and W.J. Choyke. Photoluminescence of ti in four sic polytypes. *Physical Review B*, 1974.

[26] R. Sauer, J. Weber, and J. Stolz. Dislocation-related photoluminescence in silicon. *Appl. Phys.*, 1985.

[27] T. Sekiguchi and K. Sumino. Cathodoluminescence study on dislocations in silicon. *J. Appl. Phys.*, 1995.

[28] W. Staiger, G. Pfeiffer, K. Weronek, A. Höpner, and J. Weber. Dislocation-induced defect levels in silicon. *Materials Science Forum*, 1994.

[29] M. Suezawa, Y. Sasaki, and K. Sumino. Dependence of photoluminescence on temperature in dislocated silicon crystals. *Physica Status Solidi*, 1983.

[30] H. Sugimoto, K. Araki, M. Tajima, T. Eguchi, I. Yamaga, M. Dhamrin, K. Kamisako, and T. Saitoh. Photoluminescence analysis of intragrain defects in multicrystalline silicon wafers for solar cells. *Journal of Applied Physics*, 2007.

[31] Hiroki Sugimoto, Masaaki Inoue, Michio Tajima, Atsushi Ogura, and Yoshio Ohsita. Analysis of intra-grain defects in multicrystalline silicon wafers by photoluminescence mapping and spectroscopy. *Japanese Journal of Applied Physics*, 2006.

[32] M. Tajima, M. Tokita, and M. Warashina. Photoluminescence due to oxygen precipitates distinguished from the d-lines in annealed si. *Materials Science Forum*, 1995.

[33] I. Tarasov, S. Ostapenko, C.Haessler, and E.-U. Reisner. Spatially resolved defect diagnostics in multicrystalline silicon for solar cells. *Elsevier Science S.A*, 2000.

[34] I. Tarasov, S. Ostapenko, W. Seifert, M. Kittler, and J.P. Kaleis. Defect diagnostics in multicrystalline silicon using scanning techniques. *Elsevier Science B.V.*, 2001.

[35] A.W.C van Kemenade and S.H. Hagen. Proof of the involvement of ti in the low-temperature abc luminescence spectrum of 6h sic. *Solid State Communications*, 1974.

[36] Mt. Wagner, I.G. Ivanov, L. Storasta, J.P. Bergman, B. Magnusson, W.M. Chen, and E. Janzén. Photoluminescence upconversion in 4h-sic. *Applied Physics Letters*, 2002.

[37] J. Weber, H. Bauch, and R. Sauer. Optical properties of copper in silicon: Excitons bound to isoelectronic copper pairs. *Physical Review B*, 1982.

[38] K. Weronek, J. Weber, and R. Buchner. Origin of d-band photoluminescence in silicon. *Springer Proceedings in Physics*, 1991.

[39] G. Zoth and W. Bergholz. A fast preparation-free method to detect iron in silicon. *J. Appl. Phys*, 1990.

A Silicon energy bands

Energy	Name	Temp.	Impurity / Defect	Observed in
0.735eV	ZPL	22K	Fe contamination	[6]
0.745eV	C-N		Carbon-Nitrogen complex	[9]
0.76-0.8eV	Defect	290K	Dislocation with low contamination	[33] [34] [1]
0.77-0.78eV	D_b	4.2-295K	Oxygen impurity band	[32] [18]
0.77eV	P line	12K	C-O complex related	[9] [5]
0.780eV	$CrB^{0\Gamma}$	4.2K	CrB^0 phonon replica	[8]
0.79eV	C-O	12K	Carbon-Oxygen complex	[9] [5]
0.80eV	D1'	77K	Dislocations [1]	[33] [34]
0.812eV	D1	4.2K	Dislocation related line [1]	[12] [26] [3]
0.8160	CrB^2	4.2K	Cr-B excitation of local vibrations	[8]
0.8402	CrB^1	4.2K	Cr-B excitation of local vibrations	[8]
0.8432eV	CrB^0	4.2K	Cr-B pair no-phonon	[7] [8]
0.875eV	C-Ga		Carbon-Gallium complex	[9]
0.875eV	D2	4.2K	Dislocation related line [1]	[12] [26] [3]
0.89eV	D2'	77K	Dislocations [1]	[33] [34]
0.8-0.9eV	D_{a1}	11K	Broad background emission under D1/D2	[32]
0.91eV	H-line	12K	C-O complex related	[9] [5]
0.93eV	H-line	12K	C-O complex related	[9] [5]
0.934eV	D3	4.2K	Dislocations [2]	[12] [26] [3]
0.95eV	D3'	77K	Dislocations [2]	[33] [34]
0.953eV	D5	4.2K	Straight dislocations	[26] [38]
0.9537eV	Defect	300K	Iron precipitate	[13]
0.968eV	I^{TO+20^Γ}	26K	TO + 2 Zone center phonon	[10]
0.969eV	C-C		Carbon-Carbon complex	[9]
0.98eV	R2BB	80K	Two phonon replica of band edge emission	[3]
0.9-1.0eV	D_{a2}	11K	Broad background emission under D3/D4	[32]
1.000eV	D4	4.2K	Dislocations [2]	[12] [26] [3]
1.00eV	D4'	77K	Dislocations [2]	[33] [34]
1.0089eV	FeB^0(TO)	6K	Fe-B pair phonon replica	[23]
1.0126eV	D6	4.2K	Stacking faults	[26] [38]
1.013eV	$I^{TO+0^\Gamma+IV^a}$	26K	$TO + 0^\Gamma + IV^a$ phonon	[10]
1.014eV	Cu_0	4.2K	Copper doping	[37] [38]
1.018eV	W/I1		Radiation damage	[9]
1.0315eV	I^{TO+0^Γ}	26K	TO + Zone center phonon	[10]
1.04eV	R1BB	80K	One phonon replica of band edge emission	[3]
1.045eV	Q		4-Li atom complex	[9]
1.0504eV	FeB^2	6K	Fe-B pair contamination	[23]

Continued on next page

Table 2 – continued from previous page

Energy	Name	Temp.	Impurity / Defect	Observed in
1.051eV	I^{TO+IV^b}	26K	Inter valley phonon replica	[10]
1.0595eV	FeB^1	6K	Fe-B pair contamination	[23]
1.0692eV	FeB^0	6K	Fe-B pair no phonon	[23]
1.074eV	I^{TO+IV^a}	26K	Inter valley phonon replica	[10]
1.078	EHD	4.2K	Electron Hole Droplet dislocation-area	[11]
1.082eV	EHD_{TO}	4.2K	Electron Hole Droplet dislocation-free	[15] [11] [24]
1.0835eV	In^{TO}	30K	Indium doping TO	[10]
1.0888eV	Bi^{TO}	15K	Bismuth doping TO	[10]
1.0902eV	Al^{TO}	30K	Aluminum doping TO	[10]
1.0907eV	As^{TO}	15K	Arsenic doping TO	[10]
1.0907eV	Ga^{TO}	15K	Gallium doping TO	[10]
1.0916eV	P^{TO}	15K	Phosphorus doping TO	[10]
1.092eV	BE1	4.2K	Bound exciton	[12]
1.0921eV	Sb^{TO}	15K	Antimony doping TO	[10]
1.0970eV	I^TO/FE	26K	Transversal Optical/Free exciton	[10] [15] [11]
1.0924eV	B^{TO}	15K	Boron doping TO	[10]
1.093eV	B_{TO}	4.2K	TO phonon replica of Boron bound exciton	[30] [18]
1.1365eV	I^TA/LO/FE	26K	Transversal Acoustic/Longitudinal/FE	[15] [10]
1.1545eV	I^0	26K	No phonon	[10]
2.786eV	^48_CTi	4.2K	C line Ti isotope 48 impurity in 6H SiC	[35]
2.820eV	^48_BTi	4.2K	B^0 line Ti isotope 48 impurity in 6H SiC	[35] [36]
2.85eV	^{48}Ti	4.2K	Ti isotope 48 impurity in 4H SiC	[25]
2.861eV	^48_ATi	4.2K	A^0 line Ti isotope 48 impurity in 6H SiC	[35] [36]

Table 2: Silicon energy bands

[1]D1 and D2: It has been argued that they originate in electronic transition at the geometrical kinks on dislocations [29], point defects [26] and impurities [17] and/or from the reaction products of dislocations [27].

[2]D3 and D4 lines is generally thought to be related to electronic transition within dislocation cores [19]. In addition, it has been suggested that the D3 line most likely is a phonon-assisted replica of D4 [19].

B Sample types and procedures

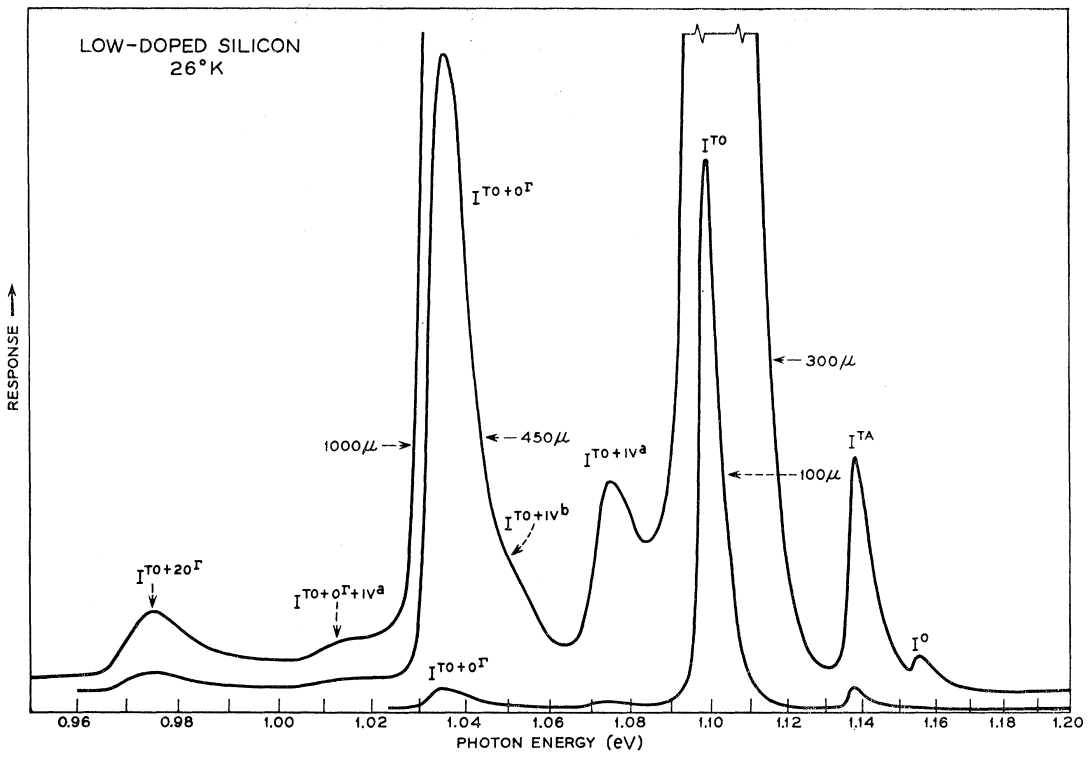

Figure 2: Low doped ($2 \cdot 10^{14} cm^{-3}$ P atoms) n-type Si PL specter from [10]

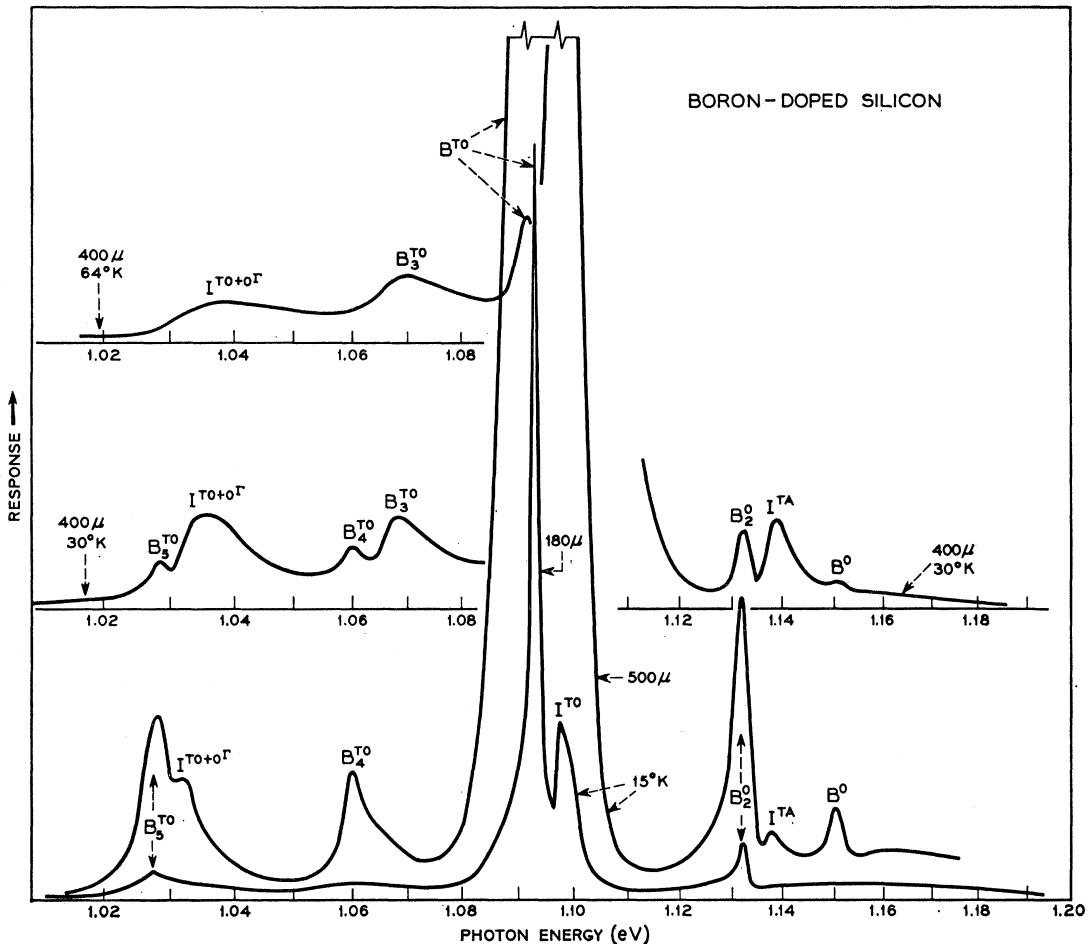

Figure 3: Boron doped ($6 \cdot 10^{16} cm^{-3}$) Si PL specter from [10]

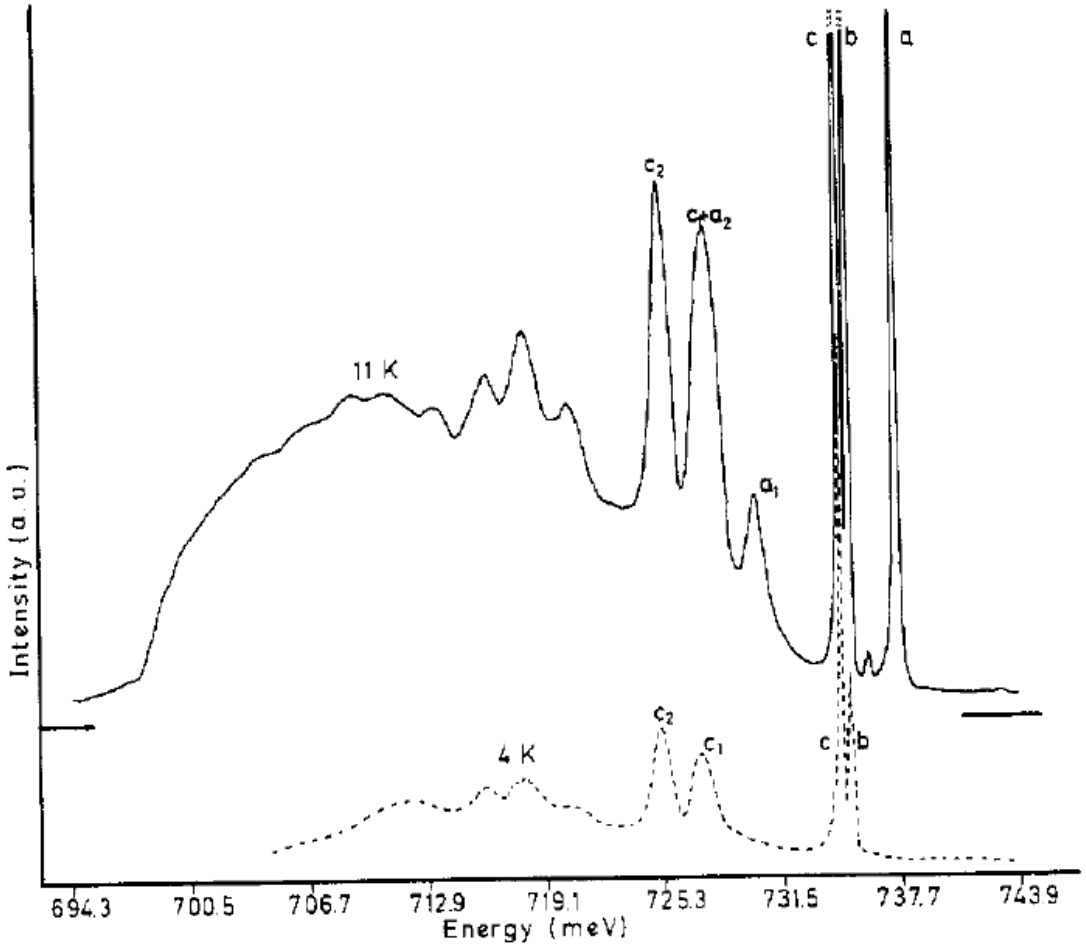

Figure 4: Iron diffused Si sample at two different temperatures from [6]

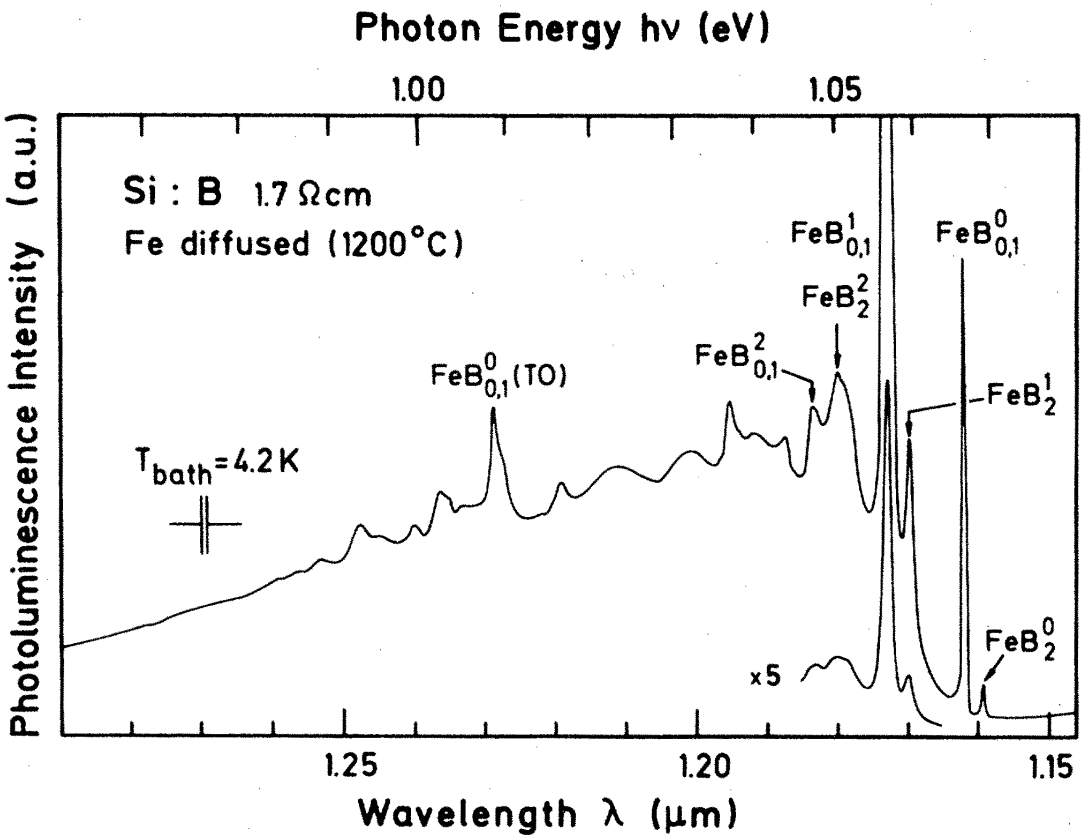

Figure 5: Iron diffused boron doped Si sample from [23]

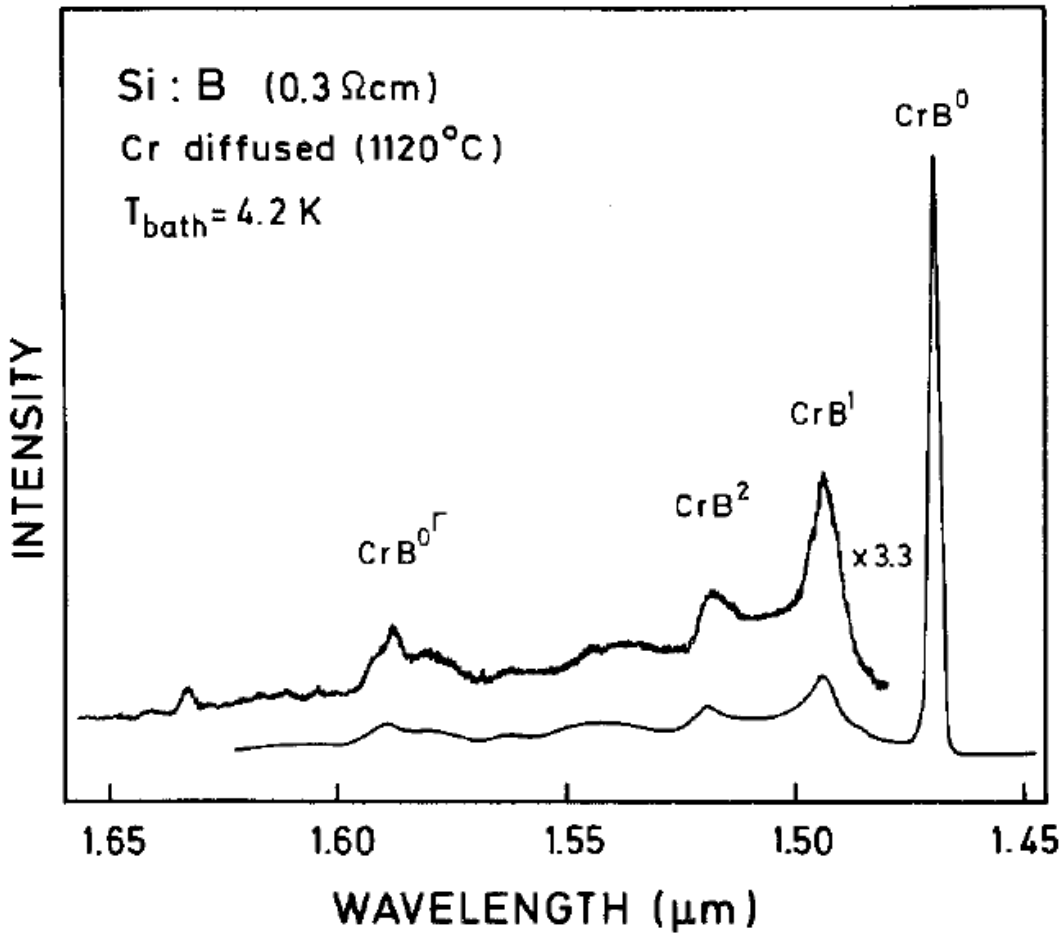

Figure 6: Chromium diffused Boron doped Si sample from [8]

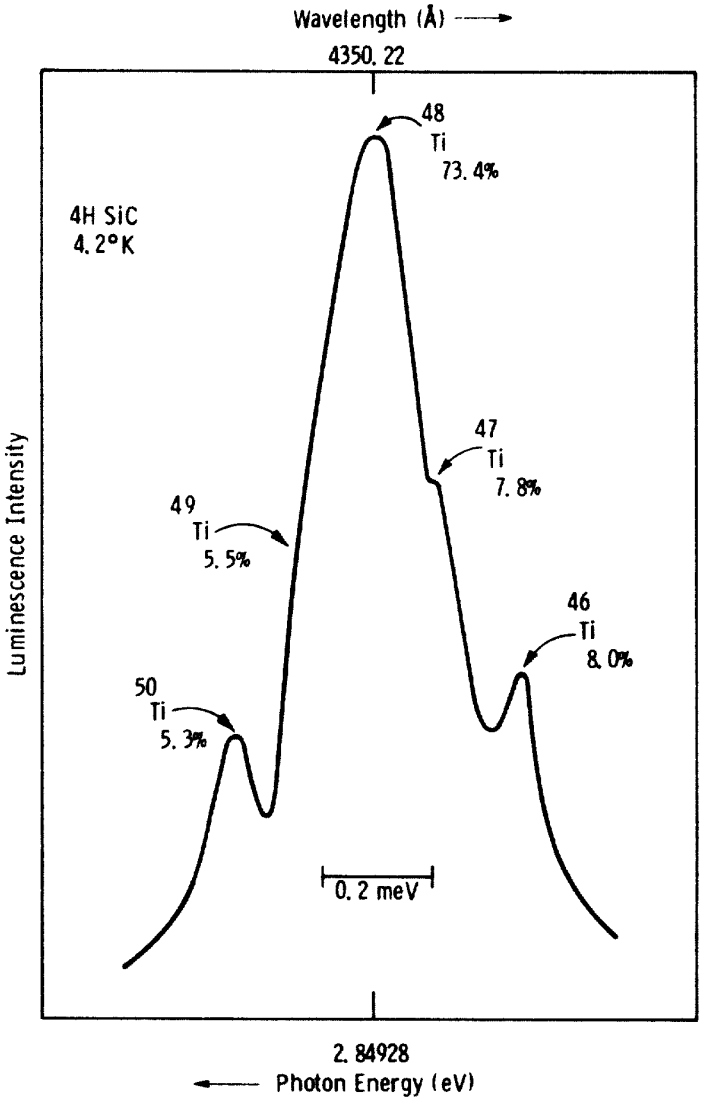

Figure 7: Titanium PL from Ti contaminated 4H SiC

Ref.	Sample type	Excitation process	Area	Processing	Doping
[30]	mc-Si	532nm Nd:YVO_4	$0.1mW/10\ \mu$m diameter	Sawing damage etched by HNO_3/HF	B-doped
[32]	Cz-Si	Kr ion laser 647nm	10 μm		Undoped
[12]	Cz-Si	Xenon lamp	50mW on 3mm modulated at 9Hz	deformed by bending at 850° C	undoped, weak n and p
[33]	mc-Si	800nm AlGaAs laser	Pulsed 300mW / 3mm		Block-casting technique for Baysix
[34]	mc-Si	800nm AlGaAs at 140mW		Produced by EFG	
[3]	mc-Si and FZ-Si	Ar ion 514nm at 300mW	100μm	Produced by EFG	boron doped $10^15cm^{-}1$
[26]	FZ-Si	Kr-ion 647nm, Ar-ion 415nm and Nd-YAG 1064nm		Deformed a 650° C and 850° C	residual 10^{12}cm^{-3} boron
[18]	mc-Si	Nd:YVO 532nm	6mW, 10μm diameter	Slicing damage etched off by HNO_3/HF	boron doped
[8]	FZ-Si and CZ-Si		50mW laser	Etched with HNO_3/HF. Chromium diffused	boron doped
[23]	FZ-Si	Ar+ 514nm	500mW	Fe diffused	boron doped
[6]	FZ-Si	Argon laser		Fe diffusion	undoped
[37]		Ar^+ 514nm at 1.5W			Cu doped
[38]	FZ-Si	Ar^+ 514nm		Heated above a Bunsen burner	Doped with Cu and/or Fe
[5]	mc-Si		6W/cm^2	Polished by HNO_3/HF	Undoped
[10]	CZ-Si	200W mercury arc 2.5eV			Undoped and doped
[11]		Ar^+ or Kr^+ laser 0.6W	0.8mm diameter	Dislocations by bending at 700°C	phosphorus doped

Table 3: Sample types and procedures